SEM Dynamic Observation of Hydrogen-Induced Cold Cracking in Weld Metal of 80 kg/mm^2 Class Steel†

Fukuhisa MATSUDA*, Hiroji NAKAGAWA** and Takeshi MATSUMOTO***

Abstract

Dynamic direct observation of hydrogen-induced cold cracking in scanning electron microscope is tried for weld metal of 80 kg/mm^2 class steel. Welded joint made with TIG-arc welding in argon-hydrogen mixing shielding gas is sliced and polished as soon as possible to minimize loss of diffusible hydrogen, and then bended with a restraint device. The specimen set to the restraint device is put into a scanning electron microscope, and crack initiation and propagation are observed and recorded with a video tape recorder. Results show close connection among degree of plastic deformation, slip bands, martensite laths and cracking mode.

KEY WORDS: (Hydrogen Embittlement) (Cold Cracking) (High Strength) (Electron Microscope) (Plastic Deformation)

1. Introduction

Weld cold cracking is one of the most serious problems in welding of high strength steel, and is well known to be hydrogen-induced delayed crack. However, its mechanism explaining the all phenomena without contradiction has not been revealed in spite of many studies. On other hand, Savage et al[1,2] discussed an interesting mechanism of hydrogen-induced crack utilizing direct dynamic observation technique of weld cold cracking with an optical microscope, in which importance of plastic deformation prior to the cracking was urged.

In observation with optical microscope, however, magnification and depth of focus are not necessarily sufficient. In these points scanning electron microscope (SEM) just has its own advantage. Actually, for example, SEM observation[3] of blister formed during cathodic charge of hydrogen make it possible to identify the crystallographic orientation of blister. Venturing to say the weak point of SEM observation, it must be difficult to detect fine slip bands due to emissive characteristic of secondary electron. So it should be necessary to understand the advantages and weak point in SEM observation.

Thus the authors in this study have tried direct dynamic SEM observation of hydrogen-induced cold cracking in weld metal of weldable high strength steel, paying attention to relation between intense plastic deformation region and cracking site.

2. Materials Used and Experimental Procedure

2.1 Material and welding procedure

Weldable high strength steel HT80 whose ultimate tensile strength is 80 kg/mm^2 class was used. The chemical composition is given in **Table 1**. About ten thin sheets,

Table 1 Chemical composition of material used

C	Si	Mn	P	S	Cu	Ni	Cr	Mo	V	B
0.13	0.27	0.86	0.011	0.004	0.25	1.08	0.50	0.43	0.04	0.0013

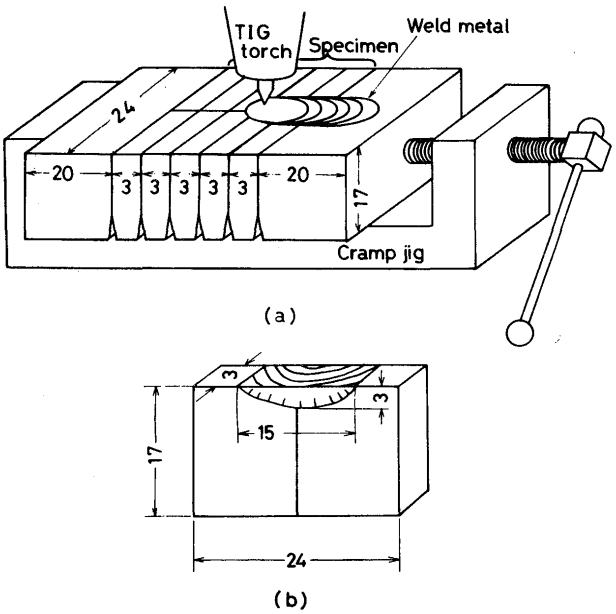

Fig. 1 Illustration of (a) welding procedure and (b) test specimen for dynamic observation

† Received on March 31, 1981
* Professor
** Research Instructor
*** Graduate Student, Osaka, Univ.

Transactions of JWRI is published by Welding Research Institute of Osaka University, Suita, Osaka, Japan

the dimensions of which were 17.5 mm in length, 12.5 mm in width and 3 mm in thickness were mechanically sliced from the material, and were gathered in two rows through two end tabs with a cramp jig as shown in **Fig. 1(a)**.

TIG-arc welding was done without filler wire along the butted line in Fig. 1 (a). Welding conditions were: welding current of 300A, arc voltage of 17V, welding speed of 150 mm/min, and shielding gas of Ar-1%H_2 in 20 l/min. The welded specimen was quenched in iced water immediately after the welding, and soon transfered into liquid nitrogen. The temperature at the middle of weld length at the quenching was about 530°C.

The welded specimen was then wedged to take the test specimens for dynamic observation whose appearance is illustrated in **Fig. 1 (b)**. The wedged test specimen was metallographically polished as soon as possible to minimize the loss of diffusible hydrogen and then set to a restraint device described nextly. It took about 4 min for the polishing.

2.2 Restraint device for observation in SEM

Figure 2 (a) and **(b)** show general view of the restraint device for dynamic observation in SEM and its principle, respectively. The device was composed of a monolithic

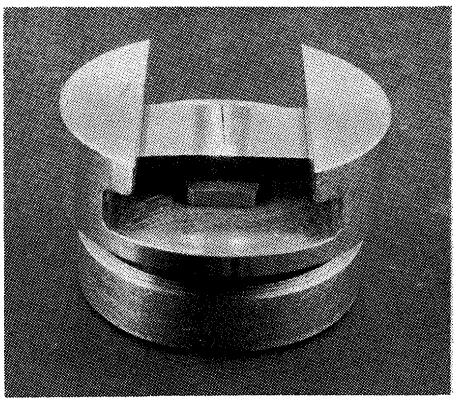

(a) general appearance

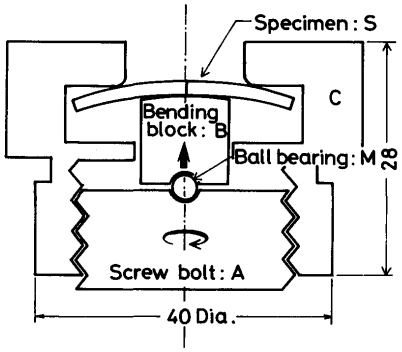

(b) principle of imposing bending strain

Fig. 2 Restraint device for dynamic observation in SEM

frame C, a screw bolt A, a ball bearing M and a bending block B. The bending block was raised through the ball bearing by tightening the screw bolt, and consequently the specimen S was bended. The bending strain was converted from the height of the raised bending block which was measured with a dial gauge. Mainly 0.8% strain was selected, because the strain more than 0.8% caused cracking during evacuating the chamber of SEM, and because the strain less than 0.7% seldom caused cracking within 2 to 3 hr.

The test specimen set to the restraint device was put into a SEM (HITACHI HSM-2B) where a TV scanning equipment (HITACHI S5010) was especially supplemented. Available magnification range was from x100 to x5000. Accelerating voltage of 20 kV, specimen current of 1 nA and working distance of 30 mm were utilized. Positional relation of the test specimen as respects incident electron beam and detector of secondary electron is shown in **Fig. 3**. After about 3 min necessary for evacuating the specimen chamber of SEM, dynamic observation was started, and video pictures were recorded with a video tape recorder and a video timer.

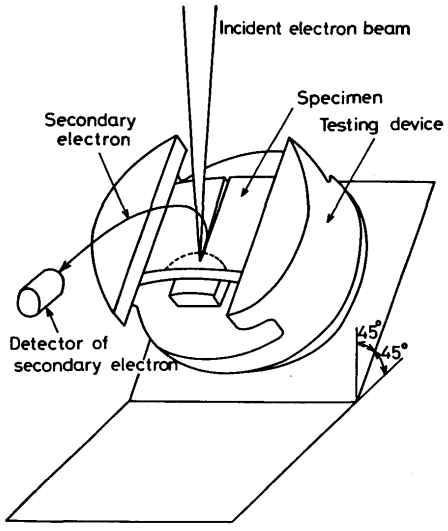

Fig. 3 Positional relation among specimen, incident electron beam and detector of secondary electron

3. Experimental Results and Discussion

3.1 Macroscopic aspect of crack initiation and propagation

Figure 4 shows an illustration of general macroscopic mode of crack initiation and propagation to facilitate the understanding of their microscopic behavior. Broken line

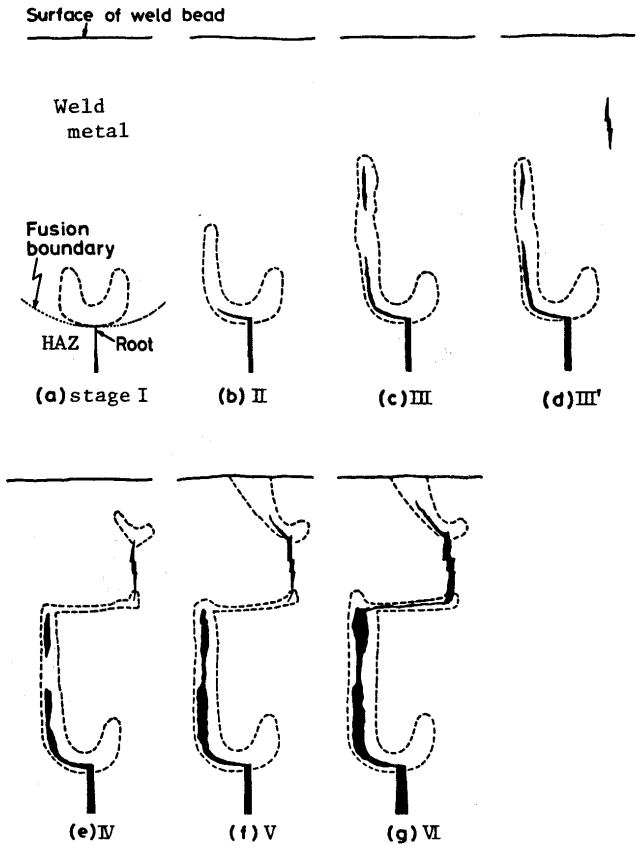

Fig. 4 Macroscopic mode of crack initiation and propagation (Broken line shows outline of intense plastic strain region)

means outline of intense plastic strain region which could be detected by SEM observation. (As well known, SEM image cannot reveal mild plastic strain region where ruggedness is not large due to emissive characteristic of secondary electron.) At first, an intense plastic strain region was formed in two direction from the root which had a role of notch (stage I). A microcrack occurred in generally either direction (stage II), though two cracks occurred in both directions on rare occasion. Even if two cracks occurred, only either of them developed. When the crack developed to some extent, a new crack occurred in the intense plastic strain region in front of the developing crack (stage III), or a new crack occurred irrespective of the intense plastic strain region (stage III'). Further they developed (stages IV and V), and finally combined into one macrocrack (stage VI). This process generally finished within about 20 min.

3.2 Microscopic observation

3.2.1 Stages I and II

Figure 5 (a) and **(b)** give examples of stages I and II, respectively, where the six letters at lower site in the video picture show the time after the start of bending in a manner as XX(hr) XX(min) XX(sec). Many bright stripes are considered to be large slip bands, and the outline of the whole bright stripes, namely the intense plastic strain region deveopled in two direction from the tip of root gap R as expected from theory of plasticity. Each slip band, however, was generally parallel to laths of martensite according to metallographic investigation of etched microstructure after the observation. In Fig. 5 (b) initiation of a microcrack C was observed.

(a) intense plastic strain region developed from root (stage I)

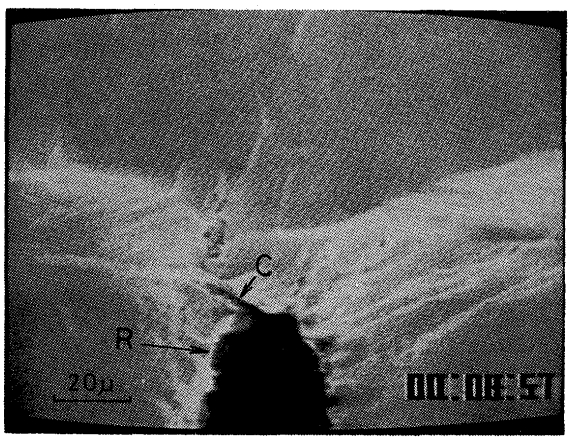

(b) crack initiation from root (stage II)

Fig. 5 Examples of stage I and stage II

3.2.2 Stages III and III'

Sequence of video pictures in **Fig. 6** gives an example of stage III. Bright stripes stretching obliquely in Fig. 6 (a) were slip bands in intense plastic strain region in front of the preceding crack which was growing in the lower zone of Fig. 6 (a). Microcracks A, B, C, D, E, F, G and H occurred one after another mainly along slip bands parallel to laths of martensite, and partly along slip bands across the laths in Fig. 6 (a) to (f). Generally crack path along the laths seems to have a tendency to occur in the first place. These microcracks finally combined into one as seen in **Fig. 7 (a)**. Etched microstructure adjacent the crack, **Fig. 7 (b)**, clearly shows characteristic of alternate crack paths along and across the laths. The fracture surface, **Fig. 7 (c)**, was quasi-cleavage mode with many tiny shallow dimples.

Sequence of video pictures in **Fig. 8** gives an example of stage III'. Intense plastic strain region developed from crack A toward upper left direction (Fig. 8 (a)). Then crack B suddenly occurred at a distance from the intense

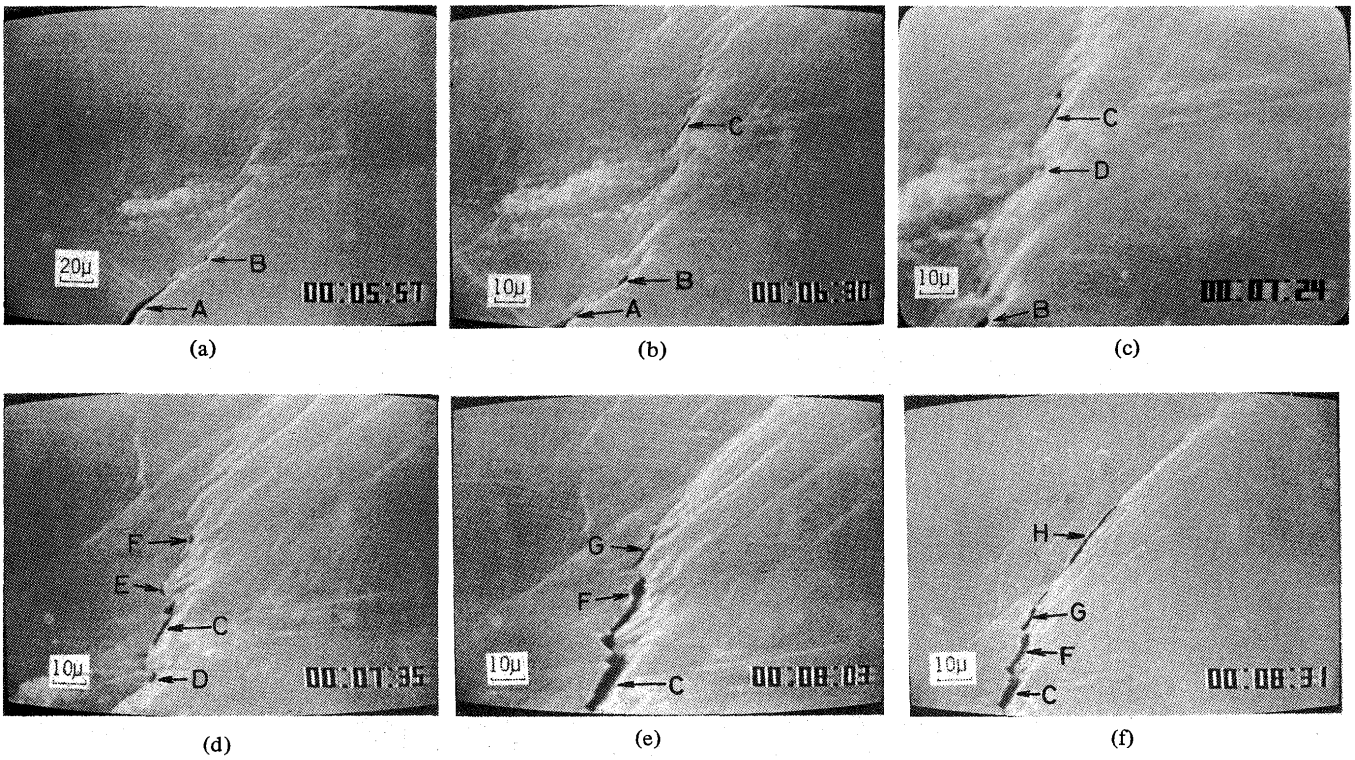

Fig. 6 An example of sequence of video pictures in stage III

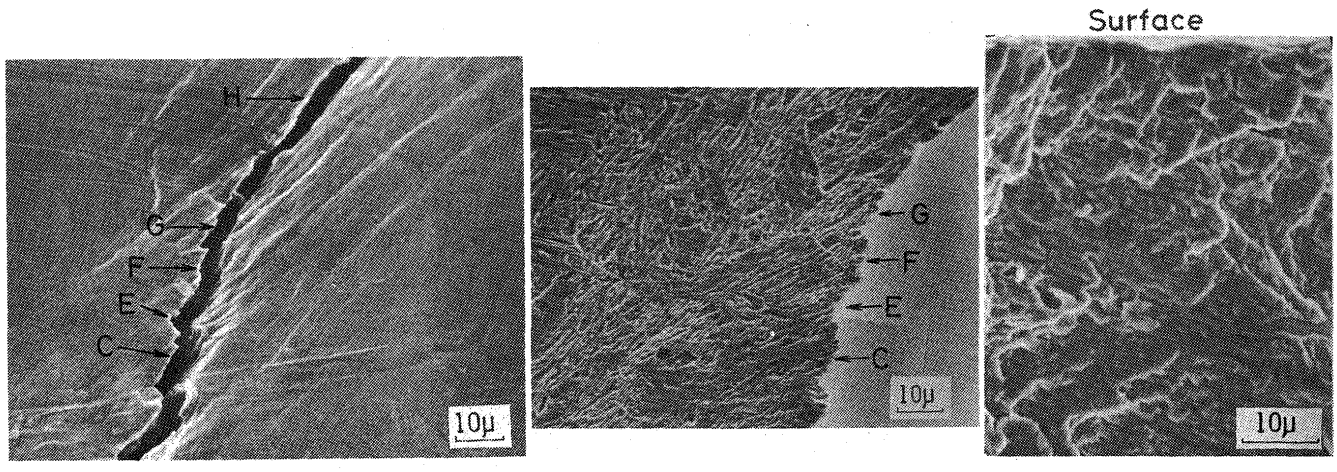

Fig. 7 Crack path and mode of fracture surface in stage III shown in Fig. 6

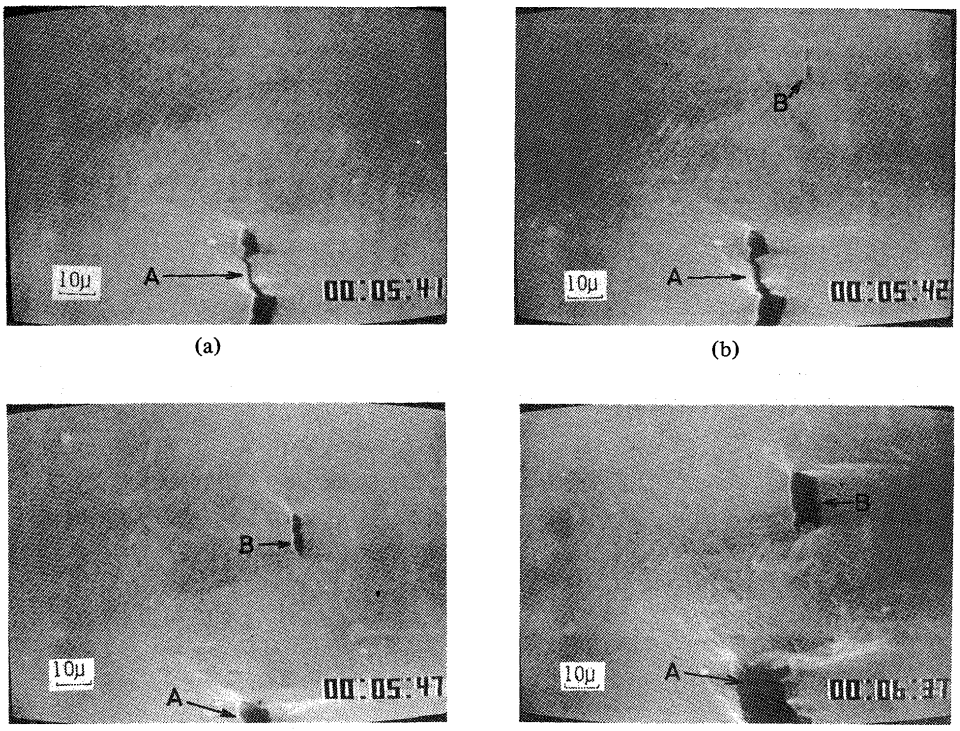

(a) (b) (c) (d)

Fig. 8 An example of sequence of video pictures in stage III'

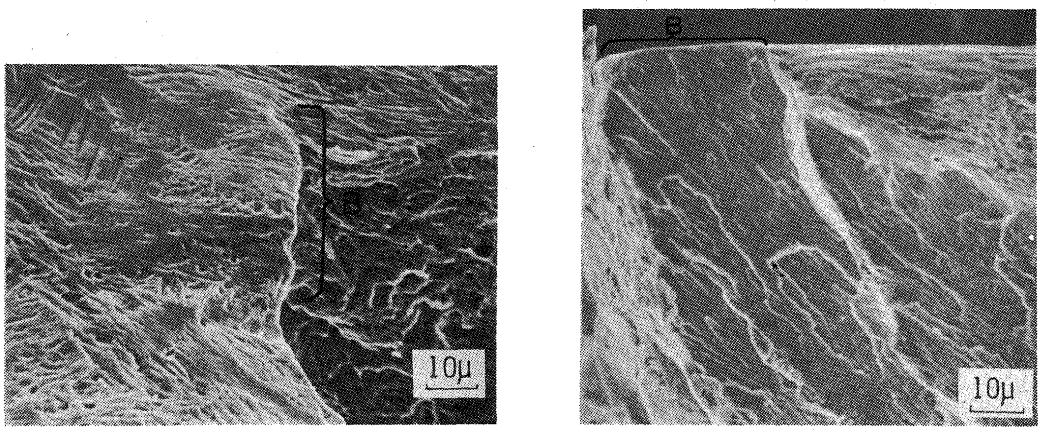

(a) (b)

Fig. 9 (a) Crack path and (b) mode of fracture surface in stage III' shown in Fig. 8

plastic strain region (Fig. 8 (b)). Together with increase in the opening of the crack B intense plastic strain regions developed from both ends of crack B (Fig. 8 (c) and (d)). Etched microstructure adjacent the crack B, **Fig. 9 (a)**, shows that the crack occurred mainly across the laths, and the fracture surface, **Fig. 9 (b)** , was quasi-cleavage mode with distinct river patterns. Judging from the direction of the river patterns, the crack occurred inside the specimen and grew toward the surface. Another characteristic of stage III' was that the crack could be easily distinguished from its surroundings on the fracture surface by dimple region.

Thus there was large difference between stages III and III' in cracking mode.

3.2.3 Stage IV

In stage IV microcracks already discribed and the intense plastic strain region around them gradually developed.

3.2.4 Stages V and VI

In these stages, crack developed in very intense plastic strain region between two cracks which had already occurred. Sequence of video pictures in **Fig. 10** gives an example. Crack A in Fig. 10 (a) was one of the two cracks which had already occurred. While the growth of the crack A was stopped, the crack opening and its intense plastic strain region developed, Fig. 10(b). The crack A in Fig. 10(c) started to grow again and another microcrack B occurred. The crack A in Fig. 10(d) grew still more, and a new crack C occurred in front of A in Fig. 10(e). The cracks A and C grew to link each other in Fig. 10(f). The characteristic of these stages was that the slip bands were not straight, but very wavy. In other words, plastic strain was very large. The fracture surface, **Fig. 11**, was shear dimple mode.

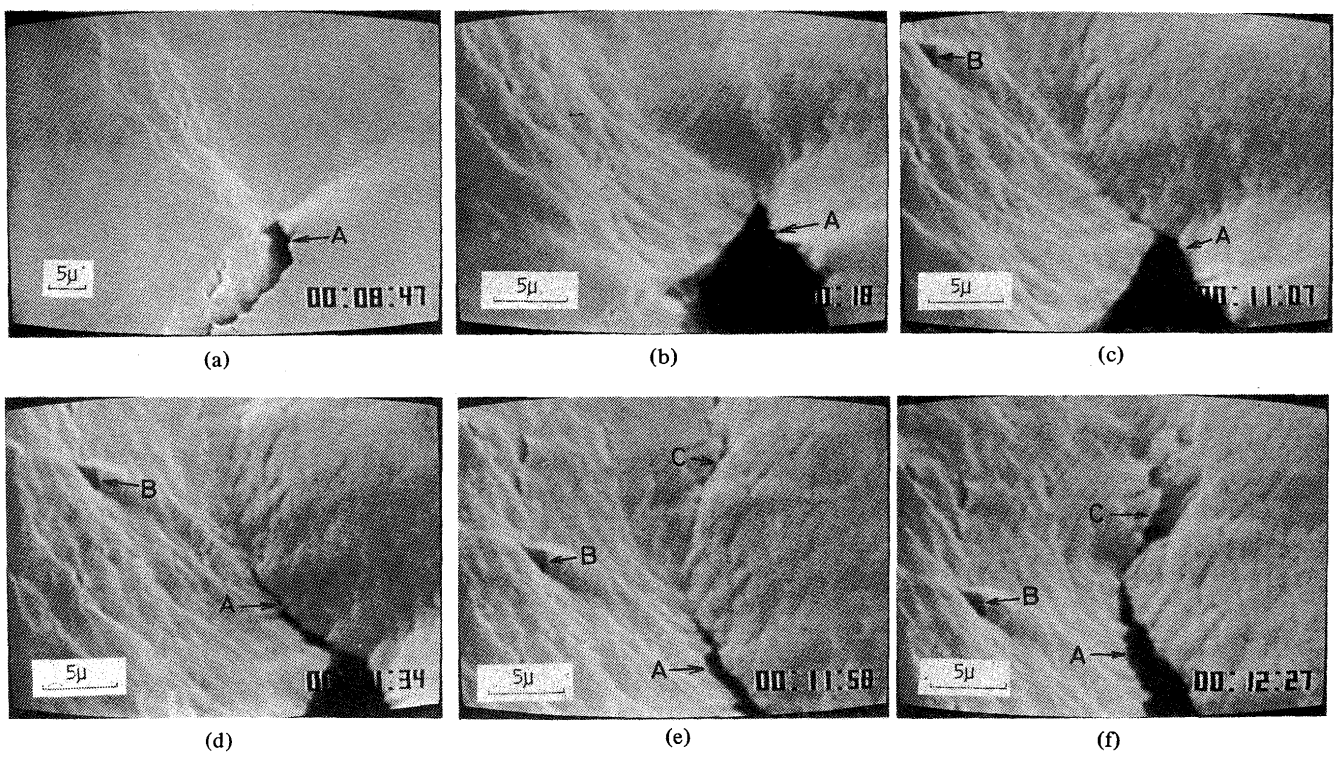

(a) (b) (c)

(d) (e) (f)

Fig. 10 An example of sequence of video pictures in stage V or stage VI

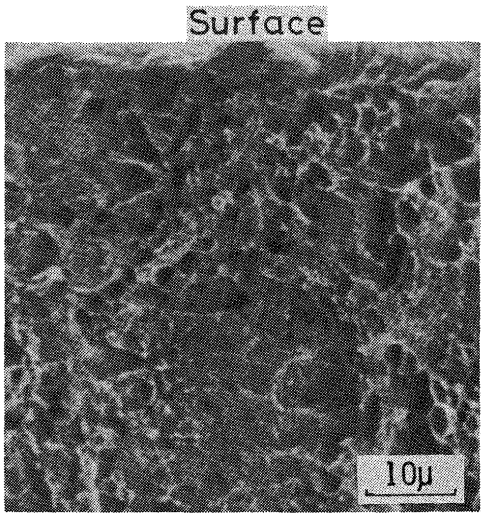

Fig. 11 Fracture surface of stage V or stage VI shown in Fig. 10

3.3 Discussion

As well known, strain (stress) and accumulation of hydrogen are necessary to hydrogen-induced crack. In stage III definite plastic strain region developed in front of growing crack, where the plastic strain was not uniform but mainly restricted to slip bands along laths of martensite. Thus it is considered that accumulation of hydrogen to such strain-concentrated parts as slip bands along the laths caused stage III crack. Since the slip bands along the laths are comparatively large, the fracture surface showed quasi-cleavage mode with dimples.

In stage III' plastic strain at the site where a microcrack should occur was not so large that could be detected with SEM. Nomarski interference microscope, however, could reveal definite plastic strain which was composed of comparatively small slip bands along laths[4]. Under this situation high concentration of hydrogen must have been

necessary to cracking, though the reason why the concentration at this site can increase is incomprehensive. It is considered that these caused definite quasi-cleavage mode without dimples.

In stages V and VI very intense plastic strain region developed between preexisting cracks, and thus the slip bands were not necessarily parallel to laths of martensite but very wavy. Since it is considered that hydrogen has a tendency to accumulate uniformly under this situation, dimple fracture mode should occur.

Besides, no intergranular crack was observed in this study. It is considered that low level of oxygen content in the weld metal with TIG-arc welding is one of the reasons for absence of intergranular crack[5].

There is an opinion[6] that interaction of hydrogen with dislocations during the formation of dislocation cells is a primary contribution for hydrogen-induced crack in pure iron. Since martensitic or bainitic structure is dominant in welded zone of root pass welding of high strength steel, corelation among orientation of laths of martensite or bainite, degree of plastic strain and slipping mode of dislocation should be studied in detail in future subject.

4. Conclusion

Dynamic observation of hydrogen-induced cold cracking with SEM has brought us interesting informations. Some different types of crack were observed and they were: (i) crack which suddenly occurred at a place where intense plastic deformation and thus slip bands were not observed. Its fracture surface showed distinct quasi-cleavage mode with river patterns. (ii) crack which occurred sporadically at slip bands along martensite laths and linked each other. Its fracture surface showed quasi-cleavage mode with many tiny shallow dimples. (iii) crack which gradually grew at a place where very wavy slip bands developed between two preexisting cracks. Its fracture surface showed shear dimple mode. Thus it was suggested that heterogenius plastic strain due to martensite lath has an important role as regards hydrogen accumulation and crack initiation.

Acknowledgement

The authors would like to thank Toray Science Foundation for finantial support.

References

1) W.F. Savage, et al: Weld. J., Vol. 55 (1976), 368s.
2) W.F. Savage, et al: Weld. J., Vol. 57 (1978), 118s.
3) T. Takeyama, et al: Proc. JIMIS-2, "Hydrogen in Metals", 1979, p. 409.
4) F. Matsuda, et al: Trans. JWRI, Vol. 8 (1979), No. 2, p. 129.
5) F. Matsuda, et al: Proc. JIMIS-2, "Hydrogen in Metals", 1979, p. 671.
6) M. Nagumo, et al: Proc. JIMIS-2, "Hydrogen in Metals", 1979, p. 405.